Research Article | Vol. 24, No. 18 | 5 Sep 2016 | OPTICS EXPRESS 20774

Optics EXPRESS

Graphene mode-locked femtosecond Cr^{2+}:ZnS laser with ~300 nm tuning range

Won Bae Cho,[1] Sun Young Choi,[2] Chunhui Zhu,[3] Mi Hye Kim,[2] Jun Wan Kim,[2] Jin Sun Kim,[1] Hyung Ju Park,[1] Dong Ho Shin,[1] Moon Youn Jung,[1] Fengqiu Wang,[3,5] and Fabian Rotermund[2,4,6]

[1]*Bio-Photonics Research Team, Electronics and Telecommunications Research Institute, Daejeon 34129, South Korea*
[2]*Department of Physics & Department of Energy Systems Research, Ajou University, Suwon 16499, South Korea*
[3]*School of Electronic Science and Engineering and Collaborative Innovation Center of Advanced Microstructures, Nanjing University, Nanjing 210093, China*
[4]*Department of Physics, Korea Advanced Institute of Science and Technology, Daejeon 34141, South Korea*
[5]*fwang@nju.edu.cn*
[6]*rotermund@kaist.ac.kr*

Abstract: Graphene has proved to be an excellent broadband saturable absorber for mode-locked operation of ultrafast lasers. However, for the mid-infrared (mid-IR) range where broadly tunable sources are in great needs, graphene-based broadly tunable ultrafast mid-IR lasers have not been demonstrated so far. Here, we report on passive mode-locking of a mid-IR Cr:ZnS laser by utilizing a transmission-type monolayer graphene saturable absorber and broad spectral tunability between 2120 nm and 2408 nm, which is the broadest tuning bandwidth ever reported for graphene mode-locked mid-IR solid-state lasers. The recovery time of the saturable absorber is measured to be ~2.4 ps by pump-probe technique at a wavelength of 2350 nm. Stably mode-locked Cr:ZnS laser delivers Fourier transform-limited 220-fs pulses with a pulse energy of up to 7.8 nJ.

OCIS codes: (140.3070) Infrared and far-infrared lasers; (140.3580) Lasers, solid-state; (140.7090) Ultrafast lasers; (160.4236) Nanomaterials; (160.4330) Nonlinear optical materials.

References and links

1. E. Garmire and A. Kost, *Nonlinear Optics in Semiconductors II* (Academic Press, 1998).
2. U. Keller, D. A. Miller, G. D. Boyd, T. H. Chiu, J. F. Ferguson, and M. T. Asom, "Solid-state low-loss intracavity saturable absorber for Nd:YLF lasers: an antiresonant semiconductor Fabry-Perot saturable absorber," Opt. Lett. **17**(7), 505–507 (1992).
3. U. Keller, "Recent developments in compact ultrafast lasers," Nature **424**(6950), 831–838 (2003).
4. S. Y. Set, H. Yaguchi, Y. Tanaka, and M. Jablonski, "Laser Mode Locking Using a Saturable Absorber Incorporating Carbon Nanotubes," J. Lightwave Technol. **22**(1), 51–56 (2004).
5. F. Wang, A. G. Rozhin, V. Scardaci, Z. Sun, F. Hennrich, I. H. White, W. I. Milne, and A. C. Ferrari, "Wideband-tuneable, nanotube mode-locked, fibre laser," Nat. Nanotechnol. **3**(12), 738–742 (2008).
6. T. Hasan, Z. Sun, F. Wang, F. Bonaccorso, P. H. Tan, A. G. Rozhin, and A. C. Ferrari, "Nanotube-Polymer Composites for Ultrafast Photonics," Adv. Mater. **21**(38â€“39), 3874–3899 (2009).
7. S. Kivistö, T. Hakulinen, A. Kaskela, B. Aitchison, D. P. Brown, A. G. Nasibulin, E. I. Kauppinen, A. Härkönen, and O. G. Okhotnikov, "Carbon nanotube films for ultrafast broadband technology," Opt. Express **17**(4), 2358–2363 (2009).
8. W. B. Cho, J. H. Yim, S. Y. Choi, S. Lee, U. Griebner, V. Petrov, and F. Rotermund, "Mode-locked self-starting Cr:forsterite laser using a single-walled carbon nanotube saturable absorber," Opt. Lett. **33**(21), 2449–2451 (2008).
9. A. Schmidt, S. Rivier, G. Steinmeyer, J. H. Yim, W. B. Cho, S. Lee, F. Rotermund, M. C. Pujol, X. Mateos, M. Aguiló, F. Díaz, V. Petrov, and U. Griebner, "Passive mode locking of Yb:KLuW using a single-walled carbon nanotube saturable absorber," Opt. Lett. **33**(7), 729–731 (2008).
10. W. B. Cho, A. Schmidt, J. H. Yim, S. Y. Choi, S. Lee, F. Rotermund, U. Griebner, G. Steinmeyer, V. Petrov, X. Mateos, M. C. Pujol, J. J. Carvajal, M. Aguiló, and F. Díaz, "Passive mode-locking of a Tm-doped bulk laser near 2 microm using a carbon nanotube saturable absorber," Opt. Express **17**(13), 11007–11012 (2009).

#268008 http://dx.doi.org/10.1364/OE.24.020774
Journal © 2016 Received 10 Jun 2016; revised 9 Aug 2016; accepted 11 Aug 2016; published 31 Aug 2016

Optics EXPRESS

11. W. B. Cho, J. H. Yim, S. Y. Choi, S. Lee, A. Schmidt, G. Steinmeyer, U. Griebner, V. Petrov, D.-I. Yeom, K. Kim, and F. Rotermund, "Boosting the Non Linear Optical Response of Carbon Nanotube Saturable Absorbers for Broadband Mode-Locking of Bulk Lasers," Adv. Funct. Mater. **20**(12), 1937–1943 (2010).
12. I. H. Baek, S. Y. Choi, H. W. Lee, W. B. Cho, V. Petrov, A. Agnesi, V. Pasiskevicius, D. I. Yeom, K. Kim, and F. Rotermund, "Single-walled carbon nanotube saturable absorber assisted high-power mode-locking of a Ti:sapphire laser," Opt. Express **19**(8), 7833–7838 (2011).
13. S. Xu, F. Wang, C. Zhu, Y. Meng, Y. Liu, W. Liu, J. Tang, K. Liu, G. Hu, R. C. Howe, T. Hasan, R. Zhang, Y. Shi, and Y. Xu, "Ultrafast nonlinear photoresponse of single-wall carbon nanotubes: a broadband degenerate investigation," Nanoscale **8**(17), 9304–9309 (2016).
14. Q. Bao, H. Zhang, Y. Wang, Z. Ni, Y. Yan, Z. X. Shen, K. P. Loh, and D. Y. Tang, "Atomic-Layer Graphene as a Saturable Absorber for Ultrafast Pulsed Lasers," Adv. Funct. Mater. **19**(19), 3077–3083 (2009).
15. W. B. Cho, J. W. Kim, H. W. Lee, S. Bae, B. H. Hong, S. Y. Choi, I. H. Baek, K. Kim, D.-I. Yeom, and F. Rotermund, "High-quality, large-area monolayer graphene for efficient bulk laser mode-locking near 1.25 μm," Opt. Lett. **36**(20), 4089–4091 (2011).
16. M. N. Cizmeciyan, J. W. Kim, S. Bae, B. H. Hong, F. Rotermund, and A. Sennaroglu, "Graphene mode-locked femtosecond Cr:ZnSe laser at 2500 nm," Opt. Lett. **38**(3), 341–343 (2013).
17. J. Ma, G. Xie, P. Lv, W. Gao, P. Yuan, L. Qian, U. Griebner, V. Petrov, H. Yu, H. Zhang, and J. Wang, "Wavelength-Versatile Graphene-Gold Film Saturable Absorber Mirror for Ultra-Broadband Mode-Locking of Bulk Lasers," Sci. Rep. **4**, 5016 (2014).
18. K. S. Kim, Y. Zhao, H. Jang, S. Y. Lee, J. M. Kim, K. S. Kim, J.-H. Ahn, P. Kim, J.-Y. Choi, and B. H. Hong, "Large-scale pattern growth of graphene films for stretchable transparent electrodes," Nature **457**(7230), 706–710 (2009).
19. I. H. Baek, H. W. Lee, S. Bae, B. H. Hong, Y. H. Ahn, D.-I. Yeom, and F. Rotermund, "Efficient Mode-Locking of Sub-70-fs Ti:Sapphire Laser by Graphene Saturable Absorber," Appl. Phys. Express **5**(3), 032701 (2012).
20. W. D. Tan, C. Y. Su, R. J. Knize, G. Q. Xie, L. J. Li, and D. Y. Tang, "Mode locking of ceramic Nd:yttrium aluminum garnet with graphene as a saturable absorber," Appl. Phys. Lett. **96**(3), 031106 (2010).
21. S. Davide Di Dio Cafiso, E. Ugolotti, A. Schmidt, V. Petrov, U. Griebner, A. Agnesi, W. B. Cho, B. H. Jung, F. Rotermund, S. Bae, B. H. Hong, G. Reali, and F. Pirzio, "Sub-100-fs Cr:YAG laser mode-locked by monolayer graphene saturable absorber," Opt. Lett. **38**(10), 1745–1747 (2013).
22. J. Ma, G. Q. Xie, P. Lv, W. L. Gao, P. Yuan, L. J. Qian, H. H. Yu, H. J. Zhang, J. Y. Wang, and D. Y. Tang, "Graphene mode-locked femtosecond laser at 2 μm wavelength," Opt. Lett. **37**(11), 2085–2087 (2012).
23. A. A. Lagatsky, Z. Sun, T. S. Kulmala, R. S. Sundaram, S. Milana, F. Torrisi, O. L. Antipov, Y. Lee, J. H. Ahn, C. T. A. Brown, W. Sibbett, and A. C. Ferrari, "2 μm solid-state laser mode-locked by single-layer graphene," Appl. Phys. Lett. **102**(1), 013113 (2013).
24. N. Tolstik, E. Sorokin, and I. T. Sorokina, "Graphene mode-locked Cr:ZnS laser with 41 fs pulse duration," Opt. Express **22**(5), 5564–5571 (2014).
25. I. T. Sorokina and E. Sorokin, "Femtosecond Cr2+-Based Lasers," IEEE J. Sel. Top. Quantum Electron. **21**(1), 273–291 (2015).
26. S. B. Mirov, V. V. Fedorov, D. Martyshkin, I. S. Moskalev, M. Mirov, and S. Vasilyev, "Progress in Mid-IR Lasers Based on Cr and Fe-Doped II–VI Chalcogenides," IEEE J. Sel. Top. Quantum Electron. **21**(1), 292–310 (2015).
27. E. Sorokin, N. Tolstik, K. I. Schaffers, and I. T. Sorokina, "Femtosecond SESAM-modelocked Cr:ZnS laser," Opt. Express **20**(27), 28947–28952 (2012).
28. N. Tolstik, O. Okhotnikov, E. Sorokin, and I. T. Sorokina, "Femtosecond Cr:ZnS laser at 2.35 μm mode-locked by carbon nanotubes," (2014), Proc. SPIE **8959**, 89591A (2014).
29. N. Tolstik, A. Pospischil, E. Sorokin, and I. T. Sorokina, "Graphene mode-locked Cr:ZnS chirped-pulse oscillator," Opt. Express **22**(6), 7284–7289 (2014).
30. R. R. Nair, P. Blake, A. N. Grigorenko, K. S. Novoselov, T. J. Booth, T. Stauber, N. M. R. Peres, and A. K. Geim, "Fine Structure Constant Defines Visual Transparency of Graphene," Science **320**(5881), 1308 (2008).

1. Introduction

In the history of solid-state laser developments, passive mode-locking utilizing saturable absorbers (SAs) is one of the most important steps for achieving ultrashort pulses. Various SAs, such as organic dyes, dye-doped solids and transition-metal-ion-doped crystals [1], have been recently proposed. Their usefulness, however, has been limited by disadvantageous factors including toxicity, low durability, and narrowband spectral coverage. In 1992, semiconductor saturable absorber mirror (SESAM) was introduced with the possibility of custom designs by controlling important parameters such as saturation fluence and recovery time for the first time [2]. The flexible parameter customization combined with robust fabrication procedures makes SESAMs widely preferred passive mode-locker for ultrashort

Optics EXPRESS

pulse generation and revolutionized ultrafast laser technology, even though they require sophisticated fabrication procedures and exhibit narrowband nonlinearity [3].

As an alternative approach to SESAMs, single-walled carbon nanotubes (SWCNTs) have emerged as broadband SAs for fiber [4–7] and bulk solid-state lasers [8–12]. The broadband characterization suggests that SWCNTs can support saturable absorption in a wide spectral range from visible to near-infrared (near-IR) up to ~2.1 μm [13]. For accessing even to longer wavelengths, two dimensional carbon nanostructures, i.e. graphene which possesses linear energy dispersion and point-bandgap structure, turned out to be a very promising absorber material [14–16]. Compared to SESAMs, graphene allows the extension of operation wavelength and the fabrication of homogeneous large-area devices [17,18]. In particular, ultrafast nonlinear optical properties of intrinsic graphene-SAs fall within a desirable range with modulation depth (about 0.5%) and saturation fluence (tens of $\mu J/cm^2$) comparable with those of SWCNT-SAs and SESAMs [3,11,15,19]. Furthermore, graphene shows superior nonlinear response times with a fast (100 - 200 fs) and a slow (1 - 1.5 ps) decay component attributed by carrier-carrier/carrier-phonon scattering and interband recombination processes [15–17,19]. By employing different types of graphene-based SAs, passively mode-locked solid-state lasers have been successfully demonstrated in various spectral regions between 0.8 and 2.5 μm [14–16,19–24].

The mid-IR wavelength range between 2 and 5 μm is frequently referred to as the "molecular fingerprint" region, as various molecules undergo robust vibrational transitions in this band [25]. Therefore, increasing demands on stable mid-IR coherent sources are driven by molecular spectroscopy and remote sensing, as well as material processing, medical and industrial applications [26]. Mid-IR solid-state lasers based on Cr^{2+}-doped ZnS and ZnSe, named "Ti:sapphire of the mid-infrared," operate between 2.0 and 3.5 μm covering an important portion of the fingerprint region [25,26]. Compared with Cr:ZnSe, the Cr:ZnS gain medium is characterized by higher thermal conductivity, higher damage threshold, better mechanical and chemical stability, and lower thermal lensing parameter *dn/dT* [25,26]. Consequently, Cr:ZnS allows the development of broadly tunable high-power femtosecond mid-IR lasers.

Passive mode-locking of Cr:ZnS lasers were recently demonstrated by utilizing different SAs, such as SESAM [27], SWCNT-SA [28] and graphene-SA [23,29]. However, the fabrication of SESAMs and SWCNT-SAs for mid-IR (> 2.5 μm) solid-state lasers is still challenging. The graphene-SA was therefore suggested as a convenient and viable candidate for developing ultrafast passive mode-lockers in the mid-IR spectral range. To date, a femtosecond Cr:ZnS laser mode-locked by a graphene-SA generated ultrashort pulses as short as 41 fs [23], highest pulse energies of up to 2.3 nJ from typical oscillator configuration [23] and 15.5 nJ from chirped pulse oscillator demanding extra-cavity pulse compression [29]. However, the broadest tuning bandwidth of about 100 nm was obtained only in the Kerr-lens mode-locking regime [26]. The combination of the high-quality graphene-SA and the excellent properties of the Cr:ZnS as gain medium is expected to significantly enhance the laser output characteristics in the mid-IR.

In this work we fabricated a transmission-type graphene-SA and studied nonlinear response of this SA in the mid-IR spectral region for the first time. The monolayer graphene mode-locked Cr:ZnS laser operating near 2.3 μm allows the generation of stable 220-fs pulses with a pulse energy of up to 7.8 nJ at a repetition rates of 112.2 MHz. By utilizing a knife and adjusting the CaF_2 prism pair used for dispersion compensation, we were able to achieve the broadest tuning bandwidth of ~300 nm in the mode-locked operation.

2. Characteristics of graphene-SA

The SA based on high-quality monolayer graphene was fabricated by employing a similar method reported in [15]. The CVD synthesized monolayer graphene on a 700-nm thick Cu foil was rapidly cooled down. Subsequently, 5 wt:% polymethyl-methacrylate (PMMA) was

Optics EXPRESS

spin-coated on the graphene as a supporting layer. By wet etching process of Cu in the 0.5 M aqueous $FeCl_3$ solution, the layer consisting of graphene and PMMA was transferred onto a 1-inch-diameter CaF_2 substrate, which is highly transmitting in the mid-IR spectral range. Finally, the PMMA supporting layer was completely removed using acetone and the fabricated monolayer graphene-SA was then ready for the mode-locking experiment.

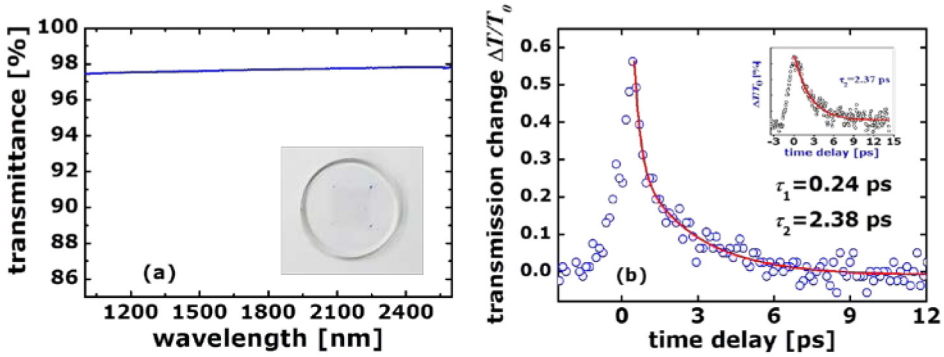

Fig. 1. Optical characteristics of monolayer graphene saturable absorber. (a) Linear transmission and photo image of graphene-SA (inset) and (b) degenerate and non-degenerate (inset) pump-probe data with fit curves measured at 2350 nm.

We investigated linear and nonlinear optical properties of the graphene-SA as shown in Fig. 1. From the linear transmission curve depicted in Fig. 1(a), the monolayer graphene-SA shows about 2.2% absorption near 2350 nm, which is similar with the theoretically expected value of $\pi\alpha \approx 2.3\%$ [30]. The inset of Fig. 1(a) shows the photo image of the monolayer graphene-SA used in the present work. Four dots on the 2-mm-thick CaF_2 substrate indicate the boundary edges of the transferred graphene layer.

The ultrafast nonlinear optical response of the graphene-SA is characterized at a wavelength near 2350 nm for the first time, providing useful insights into graphene's mid-IR optical switching capabilities. For degenerate pump-probe measurements, we used an optical parametric amplifier (OPA-SOLO, Coherent Inc.) which was pumped by a 1-kHz, 800-nm Ti: sapphire amplifier system (Libra, Coherent Inc.) delivering ~100 fs pulses. As shown in Fig. 1(b), the measured pump-probe trace shows a biexponential decay of transient absorption with an instantaneous response of 0.24 ps and a slow 1/e recovery time of 2.38 ps. To clearly verify nonlinear optical characteristics of the graphene-SA in this spectral regime, we also performed non-degenerate pump-probe experiments using 800-nm pump and 2350-nm probe, shown in the inset of Fig. 1(b). The slow decay time of the graphene-SA was revealed to be 2.37 ps, which well reproduced that of the degenerate pump-probe measurement. The recovery time constants are similar to those of graphene-SAs measured in the near-IR [15,19]. Additionally, knowledge about other essential nonlinear optical parameters such as modulation depth and saturation fluence would be desirable, but the characterization of those parameters in such a long-wavelength region remains still challenging. We are currently not able to perform nonlinear transmission and saturation measurements because of limited incident powers available from the excitation source used. However, based on nearly constant flat linear absorption above 1 μm and recent nonlinear transmission measurements at other near-IR wavelengths [15], we could expect a comparable modulation depth of about 0.4% and a saturation fluence of about 14 $\mu J/cm^2$.

3. Passive mode-locking of Cr:ZnS laser

For passively mode-locked Cr:ZnS laser with a graphene-SA, an astigmatically compensated Z-fold cavity configuration was used. The experimental setup is shown in Fig. 2(a). A diode-pumped continuous wave (CW) Er-fiber laser (IPG Photonics, linearly polarized output

Optics EXPRESS

power up to 20 W) operating at 1550 nm was used as pumping source. The pump beam waist was measured to be 1.62 mm before passing a focusing lens (L1) with a focal length of 100 mm. A 5.0-mm-thick polycrystalline Cr:ZnS crystal (IPG Photonics) with Cr^{2+} concentration of about 8.56×10^{18} cm^{-3} was used as gain medium and the crystal was mounted on a water-cooled copper block. The temperature of cooling water was stabilized at 12°C. The crystal was placed between two focusing mirrors with a radius of curvature (ROC) of −100 mm, M1 and M2. The focused pump beam waist in the laser crystal was estimated to be 30.4 μm. This allows effective mode matching with the resonator mode, whose beam waist was calculated to be from 25 to 35 μm depending on the mirror separation between M1 and M2. Two extra concave mirrors with a ROC of −75 mm, M3 and M4, shown in Fig. 2(a), formed the second cavity waist (ω_0 = 125 μm) for the transmission-type graphene-SA. This provides sufficient energy fluence for bleaching the absorption. To minimize the insertion losses, the graphene-SA was placed at the Brewster angle. The graphene-SA is movable along the beam path between M3 and M4 for varying the energy fluence by changing the beam spot size on the absorber. For achieving stable and efficient mode-locked condition, the graphene-SA was placed near the focus and the beam size ω_0 on the graphene was intended to ~135 μm. For fine tuning of the intracavity dispersion, a pair of CaF_2 prisms was inserted in the longer resonator arm containing a flat-wedged output coupler with a 15% transmission at the lasing wavelength. The graphene-SA mode-locked Cr:ZnS laser operated stably without any enclosures for isolating the laser from environmental influences such as airflow and humidity.

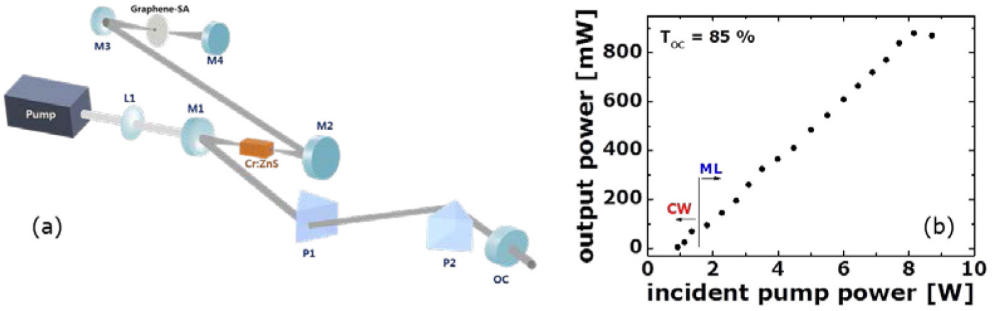

Fig. 2. (a) Schematic of the passively mode-locked Cr:ZnS laser with graphene-SA. M1 and M2, high reflective mirrors with a ROC of −100 mm; M3 and M4, high reflective mirrors with a ROC of −75 mm; OC, output coupler with 15% transmission; P1 and P2, CaF_2 prisms; Graphene-SA, monolayer graphene SA; L1, 100-mm focusing lens; Pump, diode-pumped CW Er-doped fiber laser. (b) Output power from the graphene-SA mode-locked Cr:ZnS laser. Solid vertical line indicates the mode-locking threshold.

Without intracavity dispersion compensation using the prism pair, the passively mode-locked Cr:ZnS laser produced relatively long femtosecond pulses with a pulse duration of 630 fs and a spectral bandwidth of 9.7 nm at the central wavelength of 2340 nm, yielding time-bandwidth products of 0.335 (assuming a $sech^2$-shaped pulses). The overall round-trip group-delay dispersion (GDD) of the cavity was calculated to be around + 1130 fs^2. The possible reason for measuring nearly transform limited pulses despite positive chirp is attributed to 9.5-mm-thick neutral density filters (ND) installed at the entrance of the autocorrelator. Passing the filters provides a negative dispersion of about −1710 fs^2 ($GDD_{ND\ filter}$ = −180 fs^2/mm @ 2300 nm) and acts therefore as pulse compressor outside the cavity.

For providing additional negative GDD inside the resonator and tuning the central wavelength in the mode-locked operation, we inserted a CaF_2 prism pair into the cavity, P1 and P2, in Fig. 2(a). A tip-to-tip prism separation of 280 mm, corresponding to a GDD of −2160 fs^2, was chosen to realize slightly negative net cavity GDD. The overall GDD of the resonator, therefore, was estimated to be −1030 fs^2. In this configuration, the Cr:ZnS laser

Optics EXPRESS

was stably mode-locked and output characteristics was then studied in the femtosecond mode-locked regime, as shown in Fig. 2(b). Solid vertical line indicates the mode-locking threshold, 95 mW output at 1.82 W pump power. Powers up to 880 mW was obtained in the pulsed operation at the incident pump power of 8.15 W. Higher output powers could be achieved by increasing the pump power, but strong CW components and multiple-pulsing tendency could not be suppressed. Without any signature of Q-switching instability and multiple pulsing, the laser was stably mode-locked in a whole power range above the mode-locking threshold and could be sustained for more than half day.

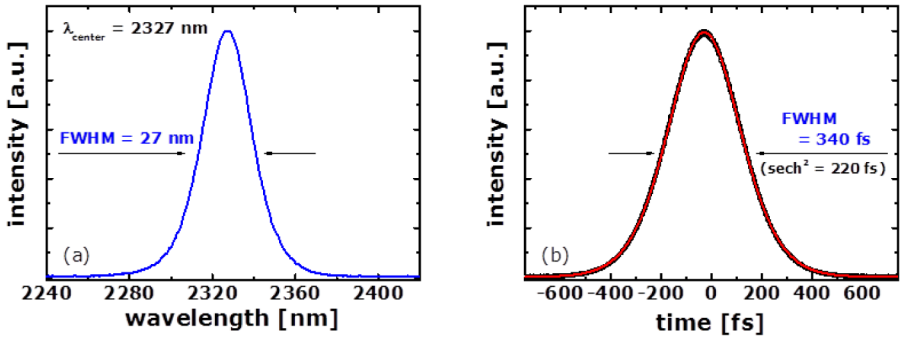

Fig. 3. Graphene-SA mode-locked Cr:ZnS laser: (a) optical spectrum and (b) autocorrelation trace.

Figures 3(a) and (b) show the output spectrum and the autocorrelation trace, measured with the WaveScan USB MIR and the PulseCheck USB MIR (A.P.E GmbH), respectively. The autocorrelation trace was fitted well by assuming a sech^2-pulse shape, yielding the pulse duration of 220 fs. The concurrently measured a spectral bandwidth of 27 nm at 2327 nm leads to a time-bandwidth product of 0.329, which is close to the transform-limited value.

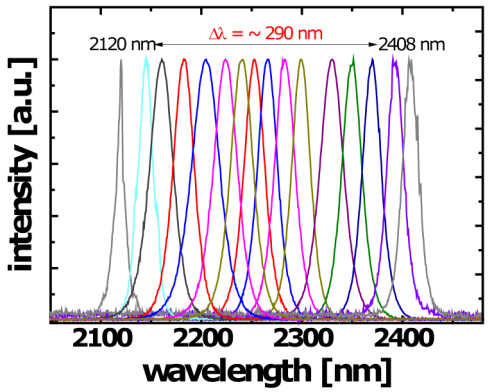

Fig. 4. Tunable laser spectra from the graphene-SA mode-locked Cr:ZnS laser.

By adjusting the second prism in combination with a knife, the central wavelength of the mode-locked Cr:ZnS laser could be tuned from 2120 to 2408 nm, as shown in Fig. 4. To the best of our knowledge, the achieved spectral tuning range of about 290 nm was the broadest one ever reported for a graphene-SA mode-locked solid-state laser. The tunability was restricted by the limited bandwidth of the dielectric coating of the intracavity mirrors, whose reflectivity was dramatically decreased below 2100 nm, and by increased atmospheric absorption above 2400 nm. In the same laser configuration but without the graphene-SA, broadly tunable CW laser operation over 650 nm was also achieved between 1950 and 2600

Optics EXPRESS

nm. Due to the spectral limitation of the spectrometer (WaveScan USB MIR), we were not able to measure additional spectra above 2600 nm.

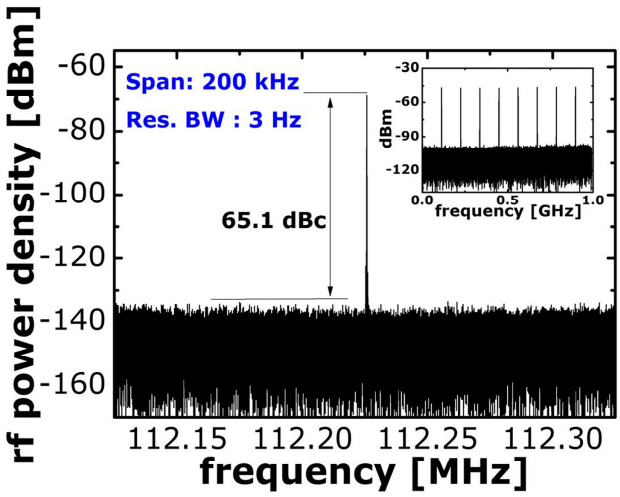

Fig. 5. Radio-frequency (RF) spectrum of the fundamental beat note at 112.22 MHz and 1 GHz wide-span RF spectrum (inset).

To verify stable mode-locked operation, we also measured radio-frequency (RF) spectra (Fig. 5). The fundamental beat note at 112.22 MHz, measured with a resolution bandwidth of 3 Hz within a 200 kHz span, exhibited a pedestal peak separation of 65.1 dB relative to carrier (dBc). The inset of Fig. 5 shows a 1 GHz wide-span RF measurement of the signal. Two RF spectra with a high extinction ratio and the absence of any specious modulation clearly indicate a stable and clean CW mode-locked operation without unwanted multiple pulsing and Q-switching modulation.

4. Conclusions

With a high-quality transmission-type graphene-SA, we demonstrated a high-performance broadly tunable femtosecond Cr:ZnS laser. In the mid-IR spectral region, nonlinear response of the graphene-SA was verified to be ~2.4 ps by degenerate and non-degenerate pump probe measurements. The mode-locked Cr:ZnS laser produced transform-limited pulses as short as 220 fs near 2330 nm. By further optimization of the laser, we expect to achieve even shorter pulse duration. In the stable single-pulse regime, average output powers up to 880 mW at 112 MHz repetition rates were achieved, resulting in a single pulse energy of 7.8 nJ. Thanks to broadband nonlinear optical characteristics of the graphene-SA, the central wavelength of the passively mode-locked Cr:ZnS laser could be tuned in a wide range of about 300 nm around 2300 nm, showing the broadest tuning range from the passively mode-locked Cr^{2+}-lasers with graphene.

Funding

This work was supported by the Creative Allied Project (CAP-15-06-ETRI) of National Research Council of Science & Technology, the National Research Foundation of Korea (NRF) Grant funded by Korea Government (MSIP) (2016R1A2A1A05005381), the Center for Advanced Meta-Materials (CAMM) funded by MSIP as Global Frontier Project (CAMM 2014M3A6B3063709), and the National Natural Science Foundation of China (61378025, 61427812).